Supporting Information for:

Comparing Ion Exchange Adsorbents for Nitrogen Recovery from Source-Separated Urine

William A. Tarpeh[†,‡], Kai M. Udert[§], Kara L. Nelson*[,†,‡]

[†]Department of Civil and Environmental Engineering, University of California, Berkeley, California 94720, United States
[#]Engineering Research Center for Re-inventing the Nation's Urban Water Infrastructure (ReNUWIt), 410 O'Brien Hall, Berkeley, California 94720, United States
[‡]Eawag, Swiss Federal Institute of Aquatic Science and Technology, 8600 Dübendorf, Switzerland

17 pages
17 equations
8 tables
13 figures

*Corresponding author: karanelson@berkeley.edu

S1. EQUATIONS

S1.1 Competitive adsorption curve fitting

Three multicomponent isotherms were fit to synthetic urine adsorption data: (1) competitive Langmuir, (2) Jain-Snoeyink, (3) and competitive Langmuir-Freundlich. These equations are written as equations 6-8 in the main manuscript. The three-solute Jain-Snoeyink model used in this study was expanded from the original Snoeyink two-solute model.[1] This model uses Langmuir isotherms but allows for different maximum adsorption densities for different cations. The interaction between solutes is competitive until the lower adsorption density is surpassed, and above this value adsorption is assumed to be non-competitive. The resulting equation for the adsorption density of each cation has a slightly different form (Equations S1-3). q_{max} and K_{ads} for each cation were from the single-cation adsorption experiments, and numerical subscripts denote each cation from lowest (1) to highest (3) maximum adsorption density. Based on q_{max} values from single-solute experiments (Table S4), ammonium was either predicted by Equation S1 (biochar, Dowex 50) or by Equation S2 (clinoptilolite, Dowex Mac 3).

$$q_{f,3} = \frac{q_{max,1}K_{ads,3}\{A_3\}}{1+K_{ads,1}\{A_1\}+K_{ads,2}\{A_2\}+K_{ads,3}\{A_3\}} + \frac{(q_{max,2}-q_{max,1})K_{ads,3}\{A_3\}}{1+K_{ads,2}\{A_2\}+K_{ads,3}\{A_3\}} + \frac{(q_{max,3}-q_{max,2})K_{ads,3}\{A_3\}}{1+K_{ads,3}\{A_3\}} \quad \text{(S1)}$$

$$q_{f,2} = \frac{q_{max,1}K_{ads,2}\{A_2\}}{1+K_{ads,1}\{A_1\}+K_{ads,2}\{A_2\}+K_{ads,3}\{A_3\}} + \frac{(q_{max,2}-q_{max,1})K_{ads,2}\{A_2\}}{1+K_{ads,2}\{A_2\}+K_{ads,3}\{A_3\}} \quad \text{(S2)}$$

$$q_{f,1} = \frac{q_{max,1}K_{ads,1}\{A_1\}}{1+K_{ads,1}\{A_1\}+K_{ads,2}\{A_2\}+K_{ads,3}\{A_3\}} \quad \text{(S3)}$$

Affinity constants and maximum adsorption densities from single-solute experiments were used as inputs for the competitive Langmuir and Jain-Snoeyink models. Affinity constants were also used as inputs to the competitive Langmuir-Freundlich, but q_{max} and n were determined by nonlinear regression using the synthetic urine data. An important difference to note between the models is that the competitive Langmuir and Jain-Snoeyink models use individual q_{max} values for each cation; in contrast, the Langmuir-Freundlich uses a single maximum adsorption density for all three cations.

To predict batch adsorption in undiluted real urine, we used initial cation activities and model parameters to solve a system of six equations containing model predictions for each cation and mass balances on each cation. For example, the following six equations were solved for the competitive Langmuir model:

$$q_{f,K} = \frac{K_{ads,K} q_{max,K} \{A_K\}}{1 + K_{ads,K}\{A_K\} + K_{ads,Na}\{A_{Na}\} + K_{ads,N}\{A_N\}} \quad \text{(S4)}$$

$$q_{f,Na} = \frac{K_{ads,Na} q_{max,Na} \{A_{Na}\}}{1 + K_{ads,K}\{A_K\} + K_{ads,Na}\{A_{Na}\} + K_{ads,N}\{A_N\}} \quad \text{(S5)}$$

$$q_{f,N} = \frac{K_{ads,N} q_{max,N} \{A_N\}}{1 + K_{ads,K}\{A_K\} + K_{ads,Na}\{A_{Na}\} + K_{ads,N}\{A_N\}} \quad \text{(S6)}$$

$$q_{f,K} = \frac{V_L}{W}(C_{0,K} - C_{f,K}) \quad \text{(S7)}$$

$$q_{f,Na} = \frac{V_L}{W}(C_{0,Na} - C_{f,Na}) \quad \text{(S8)}$$

$$q_{f,N} = \frac{V_L}{W}(C_{0,N} - C_{f,N}) \quad \text{(S9)}$$

where V_L is solution volume (L), C_0 is initial concentration of adsorbate (mg NH_4^+-N, Na^+, or K^+/L), C_f is adsorbate concentration at equilibrium (mg NH_4^+-N, Na^+, or K^+/L), W is adsorbent mass (g), and q_0 is the initial adsorption density (mg NH_4^+-N, Na^+, or K^+/g adsorbent). The same process was used for Jain-Snoeyink and Langmuir-Freundlich, with the appropriate model equations instead of equations S4-S6. Pitzer coefficients were used to convert concentration to activity (Equation 4, main manuscript). The six unknowns were the equilibrium adsorption density and concentrations of each cation.

The sum of squared errors (SSE, Equation S10) and average relative error (ARE, Equation S11) were used to compare the fit of each model to experimental data; lower SSE and ARE indicate a better fit (Table S6).[2]

$$SSE = \sum_1^n (q_{f,experimental} - q_{f,model})_i^2 \qquad \text{(S10)}$$

$$ARE = \frac{100}{n} \sum_1^n \left| \frac{q_{f,experimental} - q_{f,model}}{q_{f,experimental}} \right|_i \qquad \text{(S11)}$$

In equations S1 and S2, n is the number of experimental data points and q_f is equilibrium adsorption density (mmol N/g adsorbent).

S1.2 Dubinin-Radushkevich Isotherm

Mean free energy of adsorption was determined using the Dubinin-Radushkevich isotherm for each adsorbent (Equations S12 and S13):

$$q_e = q_0 \exp\left[-\left(\frac{\varepsilon}{\sqrt{2E}}\right)^2\right] \qquad \text{(S12)}$$

$$\varepsilon = RT\, ln\left(1 + \frac{1}{C_e}\right) \qquad \text{(S13)}$$

Where q is initial (q_0) and equilibrium (q_e) adsorption density (mmol N/g adsorbent); epsilon is the Dubinin-Radushkevich isotherm constant, and E is mean free energy (kJ/mol). R is the universal gas constant, T is temperature in Kelvins, and C_e is equilibrium concentration in mg N/L.[3]

S1.3 Continuous Experiments

Breakthrough curves and elution curves were generated from continuous adsorption and regeneration experiments, respectively. Integration of both curves allowed for calculation of the mass of ammonium adsorbed or eluted. Numerical integration was performed using the trapezoid rule:

$$\int C(t)dt \approx \sum_1^n \{(BV_n - BV_{n-1}) * \frac{1}{2} * [C(BV_n) - C(BV_{n-1})]\} \qquad \text{(S14)}$$

Where n is the number of data points, BV is number of bed volumes, and C(BV) is the concentration at a given number (BV) of bed volumes. For adsorption experiments, the mass of ammonium adsorbed was proportional to the area above the ammonium breakthrough curve and below the chloride tracer curve. For regeneration, the mass of ammonium eluted is proportional to the area below the elution curve. The equations for adsorption density (Equation S15) and regeneration efficiency (Equation S16) are:

$$q = \frac{\int [C_{Cl,ads}(t) - C_{N,ads}(t)]dt}{PV * W * MW_N} \qquad \text{(S15)}$$

$$\eta_{regen} = \frac{\int C_{N,elution}(t)dt}{\int [C_{Cl,ads}(t) - C_{N},ads(t)]dt} \qquad \text{(S16)}$$

Where PV is pore volume (L/bed volume), the volume of liquid retained by a column full of resin, W is adsorbent mass (g adsorbent), q is adsorption density (mmol N/g adsorbent), and the subscripts on concentration C(t) denote adsorption or elution. Pore volume was calculated by subtracting the mass of a column full of dry resin from the same column filled with resin and distilled water.

S1.4 Calculation of cost of conventional nitrogen removal

We used Falk et al. 2013[4] to determine the cost of installing conventional nitrogen removal at a 10 MGD activated sludge wastewater treatment plant. Costs are likely to be higher for smaller treatment plants. The net present value calculated in that study was $40 million ($150 million for installing basic biological nutrient removal, $110 million for base case activated sludge). This annualized cost was divided by the 10 MGD flow rate and the 27 mg N removed/L wastewater (influent 35 mg N/L, effluent 8 mg N/L). Other assumptions made by Falk et al. include: $0.10/kWh for operational energy use, 20 year life span, discount rate = 5.0%, and escalation rates for capital, energy and non-energy inflation rates = 3.5%.

$$\frac{\$40*10^6}{yr}*\frac{1\ day}{10^7 gal}*\frac{1\ gal}{3.78\ L}*\frac{1\ yr}{365.25\ days}*\frac{1\ L\ ww}{27\ mg\ N}*\frac{1000\ mg\ N}{1\ g\ N}=\frac{\$\mathbf{0.107}}{\boldsymbol{g\ N}} \qquad \text{(S17)}$$

S2. TABLES

Table S1: Adsorbent characteristics.

Adsorbent	Particle size (mm)	Pore structure[a]	Functional Group	pKa or pHpZc[b]	Highest Reported NH_4^+ Adsorption Density (mmol N/g)
Clinoptilolite	0.42	Macroporous[c5,6]	Aluminosilicate	3.35[7]	2.19[8]
Biochar[d]	0.25-1.25	Macroporous[9]	Carboxylate	4-5	3.19[10]
Dowex 50	0.15-0.3[11]	Microporous[5]	Sulfonate	-2	1.7[12]
Dowex Mac 3	0.3-1.2[13]	Macroporous[13]	Carboxylate	5[13]	3.8[13]

[a]The cut-off between macropores and micropores is 2 nm.[9]

[b]pHpZc is the pH of point of zero charge, another common metric for surface charge in zeolite and soil literature.

[c]Clinoptilolite pore sizes vary for grains (25-100 nm is typical) and for aggregates (500 nm is typical).[6]

[d]Given its heterogeneity, biochar has been documented to vary widely in particle size, pore structure, and adsorption density.[14]

Table S2: Synthetic Urine Recipe in 1 L nanopure water. Assumes urea completely hydrolyzed, struvite and hydroxyapatite precipitated, no volatilization, and no citrate/oxalate complexation. [15]

Substance	Amount [g]	[ml]
Na_2SO_4 anhydrous	2.30	
NaH_2PO_4 anhydrous	2.10	
NaCl	3.60	
KCl	4.20	
NH4Ac	9.60	
NH_4OH solution (25% NH_3)		13.0
NH_4HCO_3	21.40	

Table S3: Composition of synthetic and real urine. Synthetic urine parameters based on recipe; real urine measured from samples used in these experiments.

	Synthetic Urine	Real Urine
pH	8.87	8.99
Total Ammonia Nitrogen (mg N/L)	7950	3820
Sodium (mg Na/L)	2560	1620
Potassium (mg Na/L)	2200	1470
Chloride (mg Cl/L)	4180	3060
Total Phosphate (mg P/L)	542	169
Total Sulfate (mg SO_4/L)	472	1680
Total Inorganic Carbon (mg C/L)	3250	1860
COD (mg O_2/L)	8000	3460

Table S4. Summary of Langmuir best fit parameters and correlation coefficients for pure salt solutions (no pH adjustment). These data were used to construct the Langmuir best fit lines in Figure 1 and the competitive Langmuir adsorption model in Figure 2a.

	q_{max} (mmol/g sorbent)			**K_{ads} (L/mmol) x 10^{-2}**			**R^2**		
Adsorbent	NH_4^+	Na^+	K^+	NH_4^+	Na^+	K^+	NH_4^+	Na^+	K^+
Clinoptilolite	3.56	2.97[a]	2.56	1.86	1.89[a]	5.05	0.887	0.896	0.772
Biochar	4.83	5.39	3.25	0.643	2.83	2.33	0.936	0.892	0.933
Dowex 50	4.98	5.71	2.87	7.60	2.43	80.2	0.922	0.988	0.887
Dowex Mac 3	9.14	9.04	3.41	0.316	0.260	0.810	0.807	0.915	0.933

[a]Two combinations of q_{max} and K_{ads} were determined from the ISOFIT model; the other was q_{max}= 15.1 mmol/g adsorbent and K_{ads}=0.208 x 10^{-2}. The tabulated combination was chosen because of its proximity to the values for the other cations.

Table S5: Values used for modeling financial feasibility. Adsorption densities are the highest values measured in undiluted real urine adsorption experiments.

Adsorbent	Cost (USD/kg sorbent)	Adsorption Density (mmol N/g sorbent)	Bulk Density (kg/L)
Clinoptilolite	0.24[16]	2.32	0.726
Biochar	0.684[17]	2.54	0.314
Dowex 50	260[18]	3.20	0.803
Dowex Mac 3	32[18]	4.07	0.75

Table S6. Summary of single-solute Langmuir best fit parameters and correlation coefficients for ammonium in pure salt solutions (pH 9), synthetic urine, and real urine. These data were used to compare isotherms for different solutions. pH 4 pure salt solutions are in the NH_4^+ column in Table S4.

	q_{max} (mmol/g sorbent)			**K_{ads} (L/mmol) x 10^{-2}**			**R^2**		
Adsorbent	pH 9	Synthetic	Real	pH 9	Synthetic	Real	pH 9	Synthetic	Real
Clinoptilolite	4.70	4.97	3.41	0.314	2.01	8.3	0.655	0.971	0.882
Biochar	3.64	5.22	4.00	0.339	0.578	5.25	0938	0.920	0.917
Dowex 50	6.61	5.90	4.78	2.23	13.2	29.1	0.897	0.898	0.900
Dowex Mac 3	9.14	9.09	8.22	0.514	1.12	5.3	0.955	0.938	0.976

Table S7: Sum of squared errors (SSE) and average relative error (ARE) between multicomponent models and synthetic urine adsorption densities from batch experiments.

Adsorbent	**Competitive Langmuir**		**Langmuir-Freundlich**		**Jain-Snoeyink**	
	SSE $(mmol/g)^2$	ARE (%)	SSE $(mmol/g)^2$	ARE (%)	SSE $(mmol/g)^2$	ARE (%)
Clinoptilolite	33.7	37.8	14.1	66.9	35.6	41.0
Biochar	11.5	85.9	36.0	473	15.6	92.0
Dowex 50	49.8	34.5	24.8	85.9	43.0	31.1
Dowex Mac 3	89.8	61.9	6.01	27.2	86.0	61.7

Table S8: Comparison of models to triplicate undiluted real urine adsorption. "Measured" is average (± SEM) of batch adsorption with undiluted urine. All adsorption densities in mmol N/g adsorbent. CL= competitive Langmuir, LF=Langmuir Freundlich, JS= Jain-Snoeyink.

		Predicted Value (% Error)		
Adsorbent	Measured	CL	LF	JS
Clinoptilolite	2.21 ± 0.09	2.16 (-2.26)	1.33 (-39.8)	2.34 (5.74)
Biochar	2.07 ± 0.01	1.87 (-9.51)	3.56 (72.0)	1.98 (-4.28)
Dowex 50	3.16 ± 0.29	2.72 (-13.8)	5.67 (79.6)	3.45 (9.34)
Dowex Mac 3	4.07 ± 0.10	3.49 (-14.3)	5.37 (31.8)	3.71 (-9.02)

S3. FIGURES

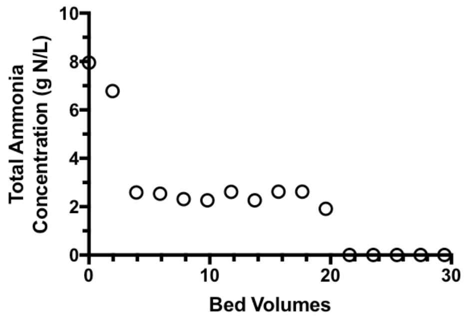

Figure S1. Elution curve for regeneration of Dowex Mac 3. The mass of ammonium eluted can be determined by numerically integrating the elution curve (Equation S1).

A) B)

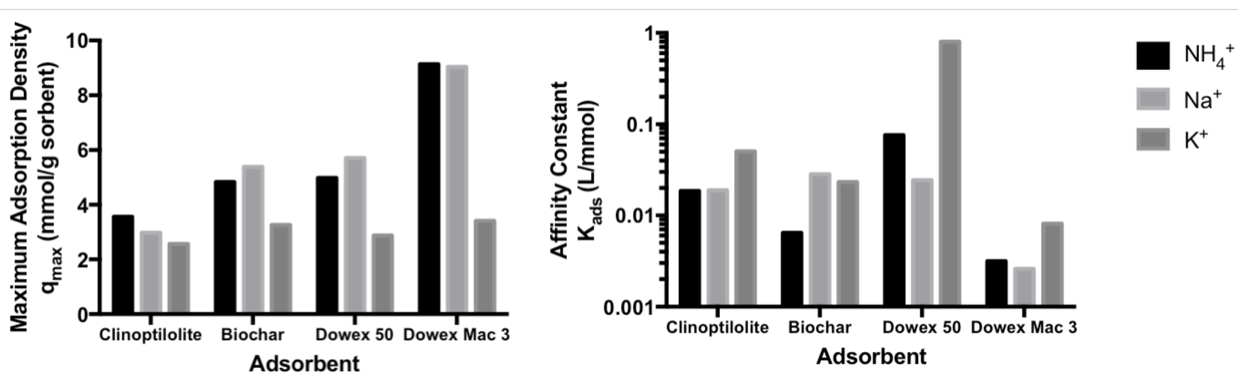

Figure S2: Comparison of Langmuir parameters (a) q_{max} and (b) K_{ads} for NH_4Cl, NaCl, and KCl without pH adjustment.

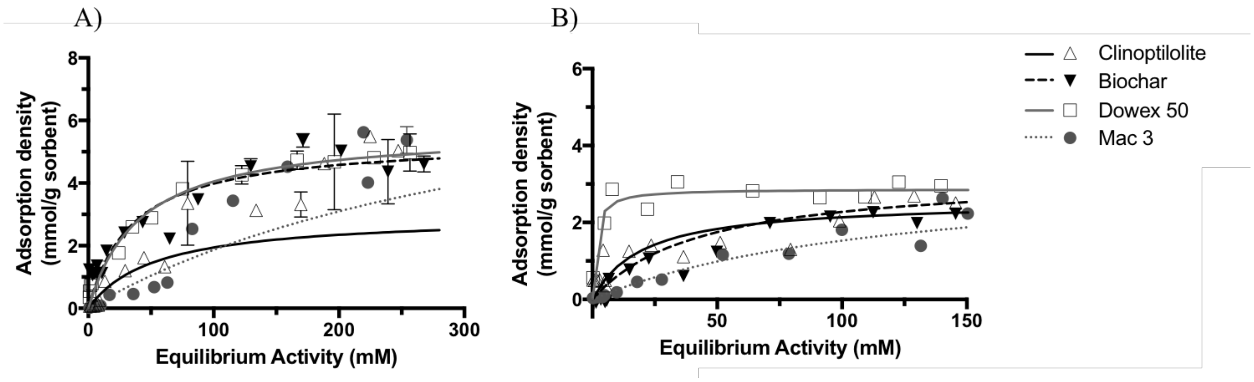

Figure S3: Adsorption for (a) NaCl and (b) KCl without pH adjustment. Error bars show dilution triplicates (n=3) for high activities (> 100 mM). Curves are Langmuir lines of best fit based on non-linear regression of experimental data. Best-fit parameters are in Table S4.

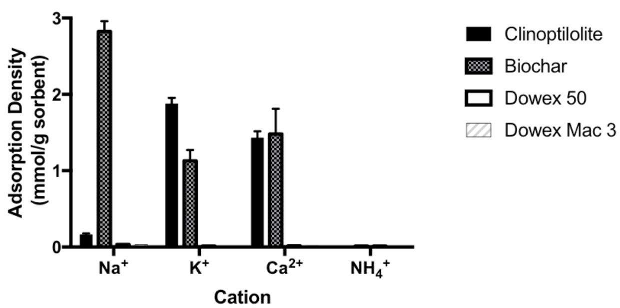

Figure S4: Estimated initial adsorption density of virgin adsorbents. Initial adsorption density was calculated based on aqueous concentrations after equilibrium with 0.65% H_2SO_4 (0.015 g adsorbent in 5 mL). Here we assumed that all cations were desorbed (q_f=0). Error bars show experimental triplicates (n=3).

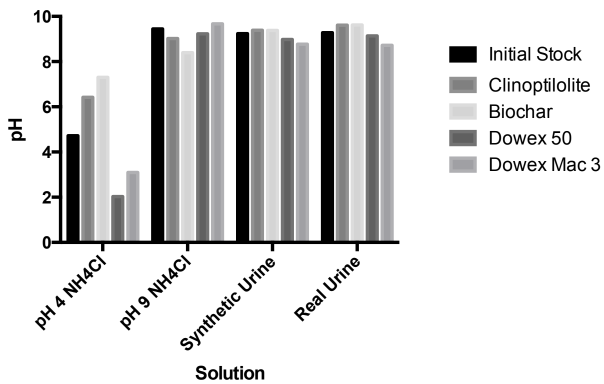

Figure S5: Comparison of pH of initial stock solutions (without adsorbent) and solution/adsorbent mixtures after 24-hour adsorption period. Results are shown for the highest concentrations tested: (i) 9000 mg N/L NH4Cl at pH 4, (ii) 9000 mg N/L NH4Cl at pH 9, (iii) undiluted synthetic urine, and (iv) undiluted real urine.

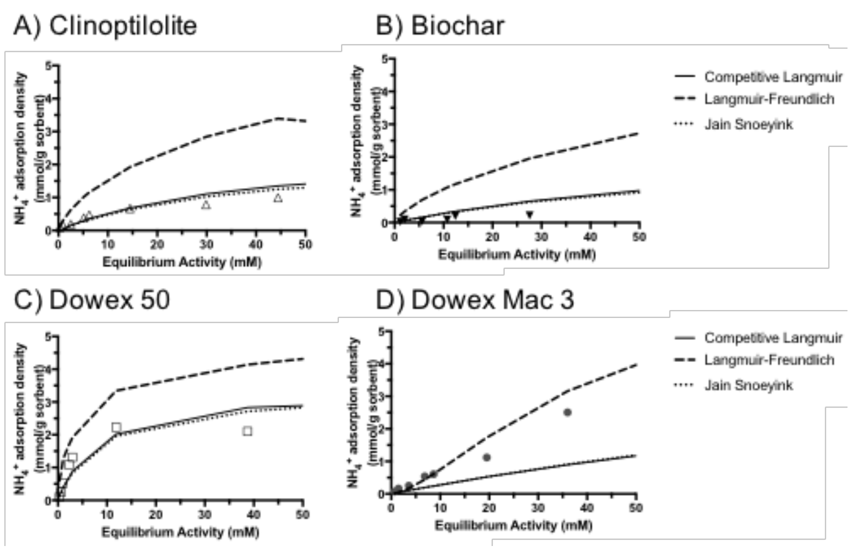

Figure S6: Comparison of synthetic urine adsorption data and competitive Langmuir, competitive Langmuir-Freundlich, and Jain-Snoeyink models for (a) clinoptilolite, (b) biochar, (c) Dowex 50, and (d) Dowex Mac 3. Data shown is for <50 mM. Full data set is in Figure 2.

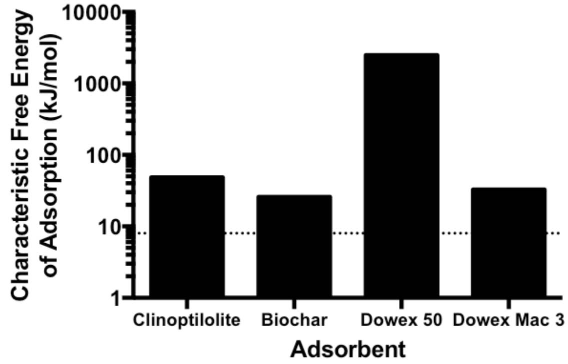

Figure S7: Free energies of adsorption determined from Dubinin-Radushkevich isotherm. If E> 8 kJ/mol (dotted line), considered ion exchange.

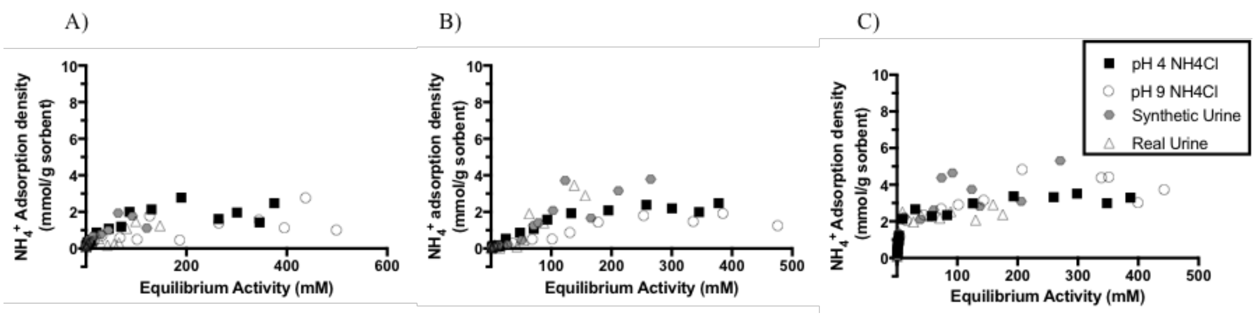

Figure S8: NH_4^+ adsorption in all solutions for (a) clinoptilolite, (b) biochar, and (c) Dowex 50.

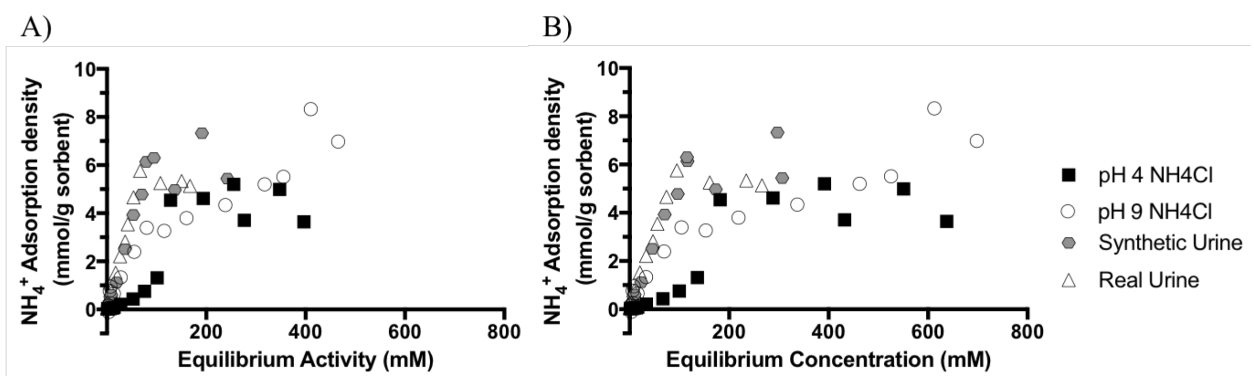

Figure S9: Comparison of adsorption curves relative to (a) activity (Figure 3b) and (b) concentration. The difference between figures can be attributed to ionic strength effects.

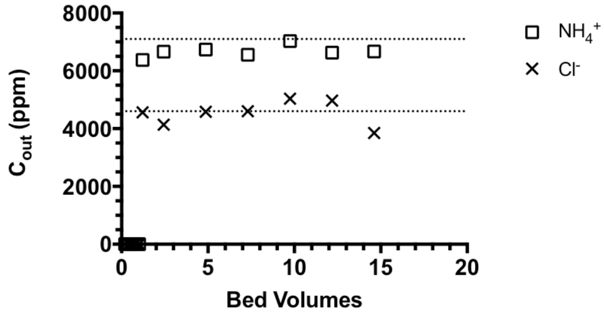

Figure S10. Ammonium and chloride concentrations in a control column with no resin. Measured concentrations are within 5% of influent concentrations (dotted lines, upper is NH_4^+, lower is Cl^-).

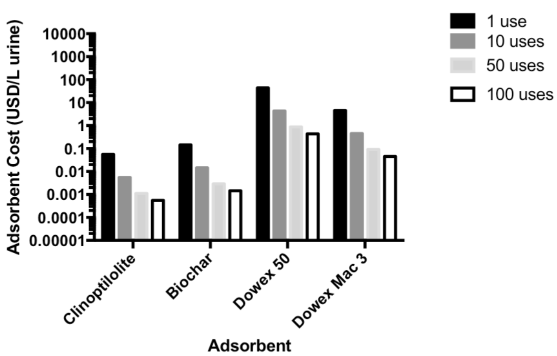

Figure S11. Recovery cost comparison of all four adsorbents (in USD/L urine) assuming 100% regeneration (r=1). Urine total ammonia concentration assumed to be 7500 mg N/L.

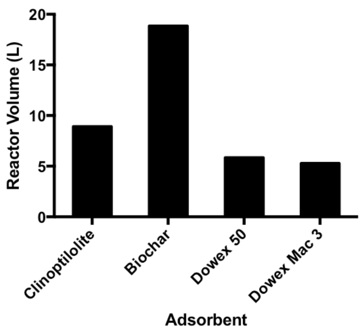

Figure S12. Required reactor volume (L) for each adsorbent based on adsorption density and bulk density. Volume of urine was 28 L, approximating the urine produced from four people in one week (1 L/person/day). Urine total ammonia concentration assumed to be 7500 mg N/L.

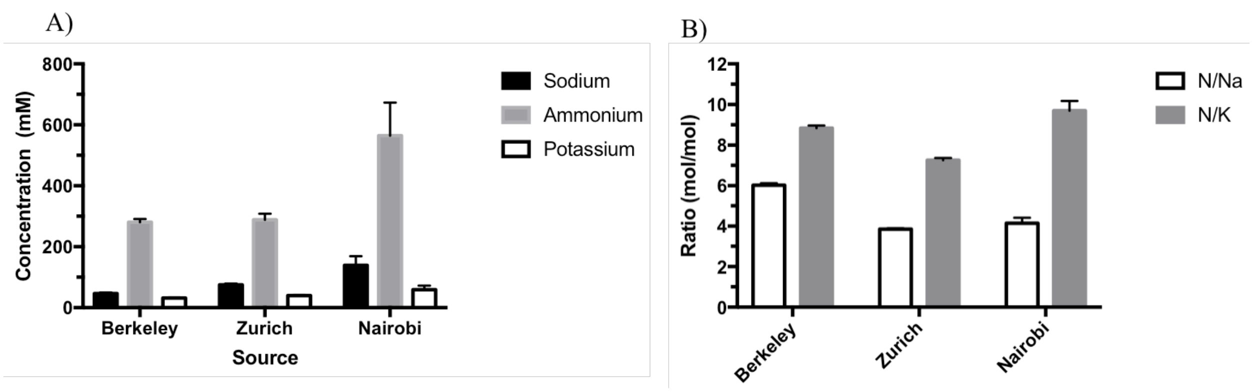

Figure S13. (a) Cation concentrations in urine collected in Berkeley, Zurich (Eawag), and Nairobi (Sanergy). (b) Cation concentration ratios from the same urine samples. Error bars reflect standard error of mean (n=5 Berkeley, n=3 Zurich, n=9 Nairobi).

REFERENCES

(1) Jain, J. S.; Snoeyink, V. L. Adsorption from Bisolute Systems on Active Carbon. *J. Water Pollut. Control Fed.* **1973**, *45* (12), 2463–2479.
(2) O'Neal, J. A.; Boyer, T. H. Phosphate recovery using hybrid anion exchange: Applications to source-separated urine and combined wastewater streams. *Water Res.* **2013**, *47* (14), 5003–5017.
(3) Foo, K. Y.; Hameed, B. H. Insights into the modeling of adsorption isotherm systems. *Chem. Eng. J.* **2010**, *156* (1), 2–10.
(4) Falk, M. W.; Reardon, D. J.; Neethling, J. B.; Clark, D. L.; Pramanik, A. Striking the Balance between Nutrient Removal, Greenhouse Gas Emissions, Receiving Water Quality, and Costs. *Water Environ. Res.* **2013**, *85* (12), 2307–2316.
(5) Jorgensen, T. .; Weatherley, L. . Ammonia removal from wastewater by ion exchange in the presence of organic contaminants. *Water Res.* **2003**, *37* (8), 1723–1728.
(6) Kowalczyk, P.; Sprynskyy, M.; Terzyk, A. P.; Lebedynets, M.; Namieśnik, J.; Buszewski, B. Porous structure of natural and modified clinoptilolites. *J. Colloid Interface Sci.* **2006**, *297* (1), 77–85.
(7) Daković, A.; Kragović, M.; Rottinghaus, G. E.; Sekulić, Ž.; Milićević, S.; Milonjić, S. K.; Zarić, S. Influence of natural zeolitic tuff and organozeolites surface charge on sorption of ionizable fumonisin B1. *Colloids Surf. B Biointerfaces* **2010**, *76* (1), 272–278.
(8) Wang, S.; Peng, Y. Natural zeolites as effective adsorbents in water and wastewater treatment. *Chem. Eng. J.* **2010**, *156* (1), 11–24.
(9) Ok, Y. S.; Uchimiya, S. M.; Chang, S. X.; Bolan, N. *Biochar: Production, Characterization, and Applications*; CRC Press, 2015.
(10) Kizito, S.; Wu, S.; Kipkemoi Kirui, W.; Lei, M.; Lu, Q.; Bah, H.; Dong, R. Evaluation of slow pyrolyzed wood and rice husks biochar for adsorption of ammonium nitrogen from piggery manure anaerobic digestate slurry. *Sci. Total Environ.* **2015**, *505*, 102–112.
(11) Hendricks, D. W. *Water Treatment Unit Processes: Physical and Chemical*; CRC Press, 2006.
(12) *DOWEX Fine Mesh Spherical Ion Exchange Resins For Fine Chemical and Pharmaceutical Column Separations*; 177-01509–904; Dow Chemical Company, Dow Water Soutions: Midland, MI.
(13) *DOWEX MAC-3 Engineering Information*; 177-01560–703; Dow Chemical Company, Dow Liquid Separations: Midland, MI, 2003.
(14) Brewer, C. E.; Chuang, V. J.; Masiello, C. A.; Gonnermann, H.; Gao, X.; Dugan, B.; Driver, L. E.; Panzacchi, P.; Zygourakis, K.; Davies, C. A. New approaches to measuring biochar density and porosity. *Biomass Bioenergy* **2014**, *66*, 176–185.
(15) Udert, K.; Larsen, T.; Gujer, W. Fate of major compounds in source-separated urine. *Water Sci. Technol.* **2006**, *54* (11–12), 413–420.
(16) Inglezakis, V. J.; Zorpas, A. A. *Handbook of Natural Zeolites*; Bentham Science Publishers, 2012.
(17) Ithaka Institute: Ayent, Switzerland, 2015.
(18) Sigma-Aldrich: St. Louis, Missouri, USA, 2015.